

Critical Flow Venturi Manifold Improves Gas Flow Calibrations

Aaron N. Johnson[†], Chunhui Li[‡], John D. Wright[†], Gina M. Kline[†], and Chris J. Crowley[†]

[†]National Institute of Standards and Technology (NIST), Fluid Metrology Group, USA
Aaron.Johnson@nist.gov (301-975-5954)

[‡]National Institute of Metrology (NIM), China

ABSTRACT

We developed a critical flow venturi (CFV) manifold that reduced the uncertainty of flow calibrations from 0.09 % to as low as 0.074 % (at a 95 % confidence level) for flows of air up to 0.84 kg/s (43 000 L/min at reference conditions of 101.325 kPa and 293.15 K). The CFV manifold also reduced the time required to complete calibrations by a factor of 10. Each CFV was installed in the manifold after it was calibrated in dry air using NIST's 677 L *PVTt* standard with an uncertainty in mass flow of 0.025%. The CFV manifold is used to calibrate customer flow meters at flows up to 21 times the flow of a single CFV. We demonstrate that interference effects between the CFVs in the manifold are negligible and we provide an uncertainty analysis of the CFV array working standard. We used the CFV array as a transfer standard to demonstrate the metrological equivalence of NIST's 677 L and 26 m³ *PVTt* standards, which agreed to better than 0.059 %.

1. Introduction

In 2009, NIST reduced the expanded mass flow uncertainty¹ of its 34 L and 677 L Pressure-Volume-Temperature-time (*PVTt*) standards by a factor of two, from 0.05 % to 0.025 %, or less [1]. Having completed upgrades to these low gas flow capabilities, we focused our attention on improving NIST's large gas flow capabilities. However, instead of improving the 26 m³ *PVTt* standard which has historically been used for gas flows above 2000 slm², a set of 21 critical flow venturis (CFVs) were 1) individually calibrated against the 677 L *PVTt* standard, and then 2) installed in a common plenum and used in parallel to extend the low uncertainty results of the 677 L *PVTt* standard to higher flows. All 21 CFVs have a nominal throat diameter of

0.5207 cm (0.205 inch), and follow the ISO 9300 toroidal throat design [2]. The CFV array spans two decades of flow from 420 slm² to 43 000 slm with an expanded mass flow uncertainty ranging from 0.074 % to 0.097 %, depending on flow. Calibrations performed with the CFV array are lower uncertainty and take less than one-tenth of the time of the 26 m³ *PVTt* standard.

This manuscript documents the calibration of the 21 CFVs using the 677 L *PVTt* standard and explains how the 21 CFVs are used together in a parallel array to calibrate customer flow meters. An uncertainty analysis is given of the CFV array working standard. Two experiments are done to demonstrate that CFV interference effects are negligible. In addition, we use the CFV array as a transfer standard to demonstrate the metrological equivalence of the 677 L and 26 m³ *PVTt* standards over 55 % of the 26 m³ *PVTt* standard flow range.

¹ The expanded uncertainty is the uncertainty at an approximate 95 % confidence level with a coverage factor of $k = 2$.

² 60 000 slm = 1 m³/s: Throughout this manuscript the units slm are *standard liters per minute* where the standardized conditions for pressure and temperature are 101.325 kPa and 293.15 K.

2. Description of the 677 L and 26 m³ PVTt flow standards

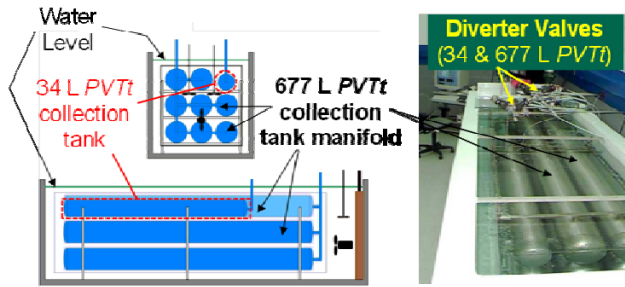


Figure 1. NIST 34 L and 677 L PVTt Standards

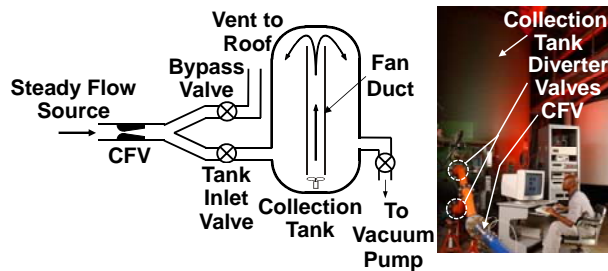


Figure 2. NIST 26 m³ PVTt Standard

Figures 1 and 2 show the 677 L and 26 m³ PVTt standards, respectively. The essential components of these standards consist of the collection tank, diverter valves (*i.e.*, bypass and tank inlet valves), a steady source of flow, a vacuum pump, and a CFV. Mass flow is measured via a timed-collection method whereby steady flow is directed into the initially evacuated collection tank for a measured time interval. At the beginning (or end) of a collection the diverter valves are actuated to start (or stop) the timer and redirect the flow into (or away from) the collection tank. The CFV plays a dual role, as it is both the flow meter being calibrated as well as a flow isolator preventing downstream pressure disturbances (caused by actuating the diverter valves) from disrupting the steady flow being measured.³ Pressure and temperature sensors (not shown in the figures) are used to determine the average pressure and temperature in the collection tank, and a chilled mirror hygrometer is

³ We operated the CFV under choked conditions. That is, we maintained the downstream-to-upstream pressure ratio across the CFV below the threshold that results in a Mach number of unity near the CFV throat location.

used to measure the mole fraction of water vapor. The average mass flow is the change in the mass in the collection tank divided by the collection time interval. The initial (or final) mass in the collection tank is determined by multiplying the initial (or final) gas density by the internal volume of the collection tank. The internal collection tank volume is determined gravimetrically prior to beginning the calibration. The initial and final gas densities are determined during the calibration process using an equation of state for air in conjunction with the measured dew point, average pressure, and temperature.

Although the 677 L and the 26 m³ PVTt standards are based on the same operating principle, the expanded uncertainty of the 677 L PVTt standard (*i.e.*, 0.025 %) is significantly lower than the expanded uncertainty of the 26 m³ PVTt standard (*i.e.*, 0.09 %) [3]. The lower uncertainty is attributed to an improved measurement of the final average gas temperature, which historically is the largest source of uncertainty of PVTt systems. The 677 L PVTt collection tank is surrounded by a thermostated water bath (see Fig. 1) enabling gas temperature measurements with uncertainties as low as 7 mK (at a 95 % confidence level). Complete descriptions of both PVTt standards and their uncertainty analyses are in previous publications [4, 5, 6].

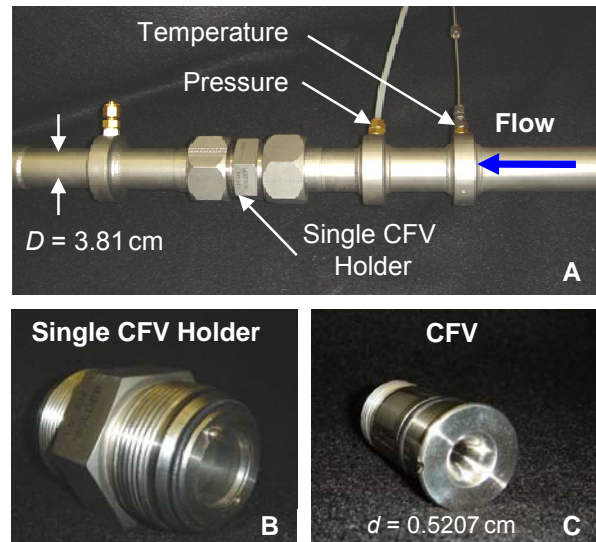


Figure 3. CFV installation used to calibrate each CFV against the 677 L PVTt standard.

3. Calibration of the 21 CFVs via the 677 L PVTt Standard

Each of the 21 CFVs was individually calibrated against the 677 L PVTt standard in the piping configuration shown in Fig. 3. The CFV in Fig. 3C is inserted into the holder shown in Fig. 3B. Next, the holder and CFV are installed in the $D = 3.81$ cm (1.5 in) pipe section shown in Fig. 3A. Calibrations were done using air dried to a dew point temperature of 256 K or less. A chilled mirror hygrometer was used to measure the dew point temperature within 0.4 K (at the 95 % confidence level). We calibrated each CFV over a pressure range from 200 kPa to 800 kPa at ambient temperatures. The locations of the pressure and temperature measurement are shown in Fig. 3A.

The calibration results are characterized by two dimensionless parameters, 1) the discharge coefficient and 2) the throat Reynolds number. The discharge coefficient is defined as

$$C_d = \frac{\dot{m}}{\dot{m}_{th}} = \frac{4\dot{m}\sqrt{R_u T_0}}{\pi d^2 P_0 C_R^* \sqrt{\mathcal{M}}} = \frac{\dot{m}\sqrt{R_u T_0}}{A P_0 C_R^* \sqrt{\mathcal{M}}}, \quad (1)$$

which is the ratio of the mass flow (\dot{m}) measured by the PVTt standard and the theoretical mass flow (\dot{m}_{th}) predicted by one-dimensional, compressible flow theory [7]

$$\dot{m}_{th} = \frac{\pi d^2 P_0 C_R^* \sqrt{\mathcal{M}}}{4\sqrt{R_u T_0}}. \quad (2)$$

Here P_0 is the upstream stagnation pressure, T_0 is stagnation temperature, C_R^* is the real gas critical flow function [8, 9], $R_u = 8314.472$ kJ/mol·K is the universal gas constant [10], \mathcal{M} is the molar mass of air, and $d = 0.5207$ cm (0.205 in) is the nominal CFV throat diameter. For this work, the throat Reynolds number is defined by

$$Re_d \equiv \frac{4\dot{m}_{th}}{\pi d \mu_0} = \frac{d P_0 C_R^* \sqrt{\mathcal{M}}}{\mu_0 \sqrt{R_u T_0}} \quad (3)$$

where μ_0 is dynamic viscosity. Both μ_0 and C_R^* are evaluated at the stagnation pressure and temperature using REFPROP [11]. The stagnation conditions are determined by

$$T_0 = T_m \left[1 + (1-r) \left(\frac{\gamma-1}{2} \right) M^2 \right] \quad (4a)$$

$$P_0 = P \left[1 + \left(\frac{\gamma-1}{2} \right) M^2 \right]^{\gamma/\gamma-1} \quad (4b)$$

where T_m is the measured temperature, P is the measured static pressure, $\gamma = C_p/C_v$ is the ratio of constant pressure to constant volume specific heats, $r = 0.75$ is the assumed value of the recovery factor which accounts for viscous heating of the gas as it stagnates against the temperature probe [2], and $M = u/a$ is the Mach number in the approach piping (*i.e.*, a ratio of the average velocity u to the sound speed a). The Mach number during calibration is determined using the measured mass flow \dot{m}

$$M = \frac{u}{a} = \frac{4\dot{m}}{\rho a \pi D^2} \quad (5a)$$

where ρ and a are the density and sound speed in the approach piping, and $D = 3.81$ cm is the diameter of the upstream piping. However, when the CFV is used as a working standard to measure flow, \dot{m} is unknown. In this case, the Mach number is calculated based on the following approximate expression [12]

$$M = \frac{1}{\beta^2} \left(\frac{2}{\gamma+1} \right)^{\frac{\gamma-3}{2\gamma-2}} \left[1 - \sqrt{1 - 2\beta^4 \left(\frac{2}{\gamma+1} \right)^{\frac{2}{\gamma-1}}} \right] \quad (5b)$$

where $\beta = d/D$.

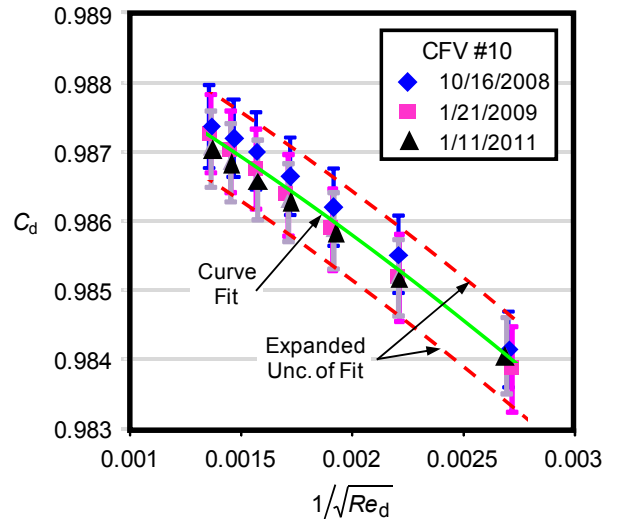


Figure 4. Calibration history of CFV 10

Table 1. Curve fit coefficients for 21 CFVs calibrated on the 677 L *PVTt* Standard

CFV # []	a_0 []	a_1 []	a_2 []	a_3 []	# of repeat calibrations []	σ_{reprd} [% , $k = 1$]	$U_e(C_{d,\text{FIT}})$ [% , $k = 2$]
1	0.98791	-0.3995	-516.373	0	5	0.033	0.087
2	0.99289	-3.08812	146.3936	0	3	0.026	0.076
3	0.99965	-2.36133	-312.791	0	4	0.034	0.088
4	0.9833	16.84098	-9468.58	1438696	4	0.029	0.084
5	0.98662	-1.46752	-190.363	0	4	0.025	0.075
6	0.98969	-1.6386	-160.272	0	3	0.012	0.061
7	0.99367	-1.75784	-284.938	0	3	0.016	0.064
8	0.98779	-1.39391	-228.755	0	4	0.019	0.068
9	0.99265	-0.50505	-553.656	0	3	0.023	0.072
10	0.98981	-1.65857	-178.45	0	3	0.016	0.064
11	0.99427	-2.0298	-147.197	0	3	0.017	0.065
12	0.99799	-2.85807	-193.763	0	3	0.033	0.087
13	0.99954	-3.3405	-29.7293	0	3	0.024	0.074
14	0.99649	-1.14449	-519.498	0	4	0.025	0.075
15	0.99357	-1.28767	-348.734	0	3	0.028	0.079
16	0.99027	-1.7053	-208.502	0	2	0.031	0.083
17	0.9950	-1.26906	-447.618	0	2	0.015	0.063
18	0.98856	-1.36847	-228.208	0	2	0.018	0.067
19	0.99303	-1.34008	-309.829	0	4	0.019	0.069
20	0.99846	-3.64953	-28.907	0	2	0.012	0.061
21	0.99883	-3.01017	-159.343	0	2	0.014	0.062

Figure 4 shows three sets of calibration data for CFV 10 (*i.e.*, one of the 21 CFVs) taken during a three year period. The C_d data is plotted as a function of the inverse square-root of throat Reynolds numbers $1/\sqrt{Re_d}$. This variable linearizes the calibration results because the boundary layer along the CFV wall is laminar and varies as $1/\sqrt{Re_d}$ for $Re_d < 10^6$. We fit the measured C_d values shown in Fig. 4 with the third degree polynomial in $Re_d^{-1/2}$

$$C_d^{\text{FIT}} = a_0 + a_1 Re_d^{-1/2} + a_2 Re_d^{-1} + a_3 Re_d^{-3/2}, \quad (6)$$

depicted by the solid line (—). The reproducibility of the three calibrations is defined to be the standard deviation of curve fit residuals, $\sigma_{\text{reprd},10} = 0.016\%$ where the subscript “10” refers to CFV 10. The expanded uncertainty of the fit is denoted by the dashed line (----) in Fig. 4. We used the method of propagation of

uncertainty [13, 14] to compute the combined standard uncertainty of the fitted discharge coefficient. All of the uncertainty components are taken to be uncorrelated so that the uncertainty is

$$\frac{u(C_d^{\text{FIT}})}{C_d^{\text{FIT}}} = \sqrt{\left[\frac{u(\dot{m})}{\dot{m}} \right]^2 + \left[\frac{u(P_0)}{P_0} \right]^2 + \sigma_{\text{reprd}}^2 + \frac{1}{4} \left[\frac{u(T_0)}{T_0} \right]^2 + \frac{1}{4} \left[\frac{u(\mathcal{M})}{\mathcal{M}} \right]^2} \quad (7)$$

where $[u(\dot{m})/\dot{m}] = 0.0125\%$ is the standard uncertainty of the measured mass flow from the 677 L *PVTt* system, $[u(P_0)/P_0] = 0.02\%$ and $[u(T_0)/T_0] = 0.03\%$ are the standard uncertainties in the stagnation pressure and temperature respectively, and $[u(\mathcal{M})/\mathcal{M}] = 0.0024\%$ is the uncertainty in the molar mass attributed mostly to the amount of water vapor in the air [1]. The uncertainties of d , R_u , and C_R^* have been taken to be zero. The parameters d and R_u do not contribute

any uncertainty as long as the same values are used both during calibration and application. Likewise, the uncertainty attributed by C_R^* is negligible provided the stagnation conditions

and gas type are the same during the calibration and application. Table 1 lists the fit coefficients, the reproducibilities, and the expanded uncertainties for all 21 CFVs.

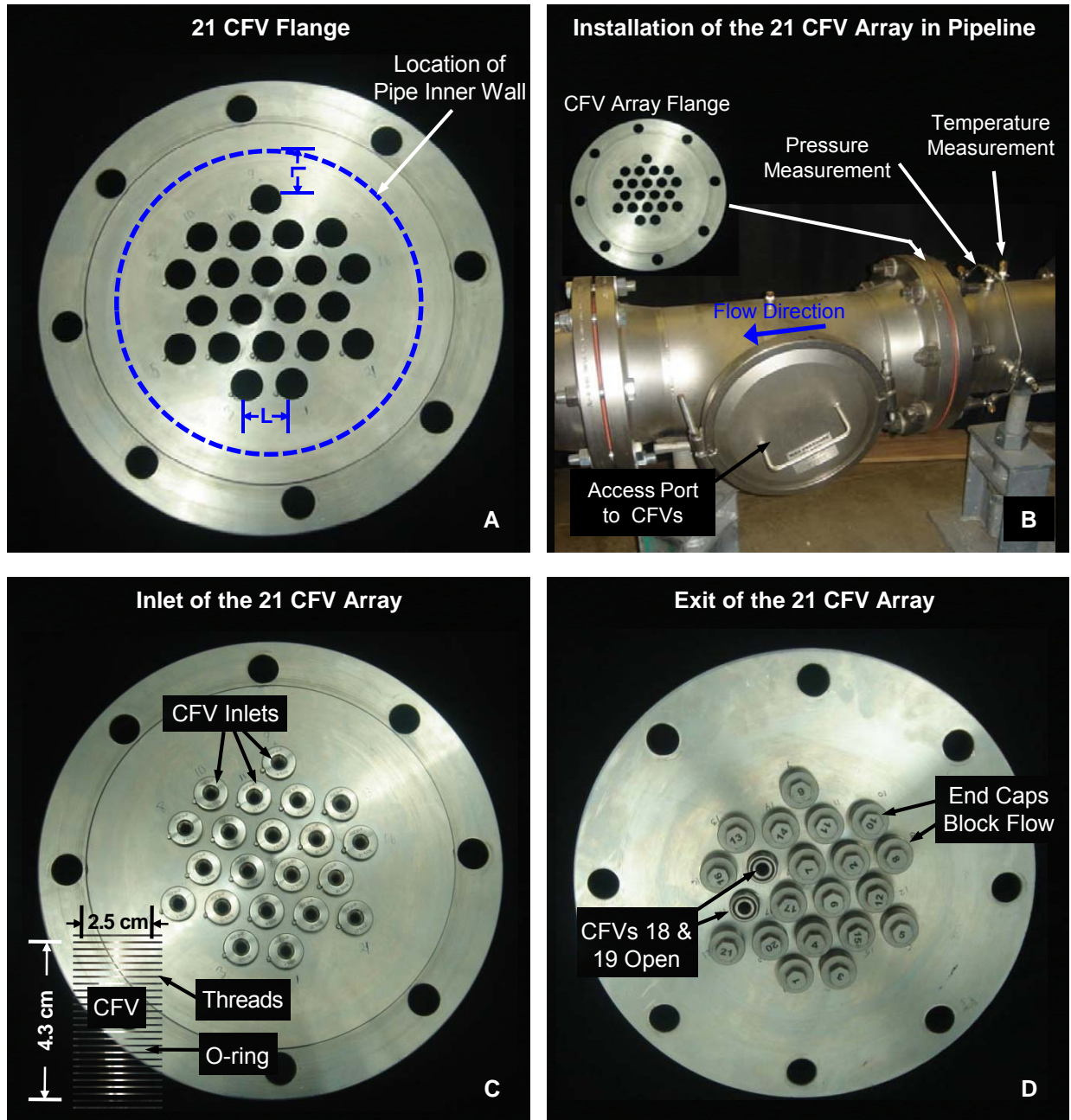


Figure 5. NIST 21 CFV Array

4. The CFV Array Working Standard

Description of the CFV Array

Figure 5A shows the 21 CFV holder which consists of a 20.32 cm (8 inch) flange having 21 apertures. The centers of adjacent apertures are separated by $L = 3.2$ cm, and no aperture is closer than $L = 3.2$ cm from the pipe interior wall. Figures 5C and 5D show the upstream and downstream side of the holder with all 21 CFVs installed. The o-ring installed on the outside of the CFV shown in Fig. 5C prevented leaks. On the downstream side of the holder, threaded caps prevented flow through selected CFVs. Figure 5D shows CFVs 18 and 19 open (*i.e.*, uncapped) while the remaining CFVs are capped. Figure 5B shows the location where the 21 CFV array was installed in the pipeline as well as the locations of pressure and temperature sensors. The average temperature is determined using three 0.3125 cm (0.125 in) diameter thermistors positioned 120 degrees apart around the pipe circumference. The mass flow through the CFVs was controlled either by changing the upstream stagnation pressure or by removing (or fastening) the CFV end caps using the access port shown in Fig. 5B.

Discharge Coefficient for a CFV Array

Equation 1 defines the discharge coefficient for a single CFV. An analogous expression for multiple CFVs installed in parallel is

$$C_{d,array} = \frac{\dot{m}_{array}}{\dot{m}_{th,array}} = \frac{\dot{m}_{array} \sqrt{R_u T_0}}{A_{array} P_0 C^* \sqrt{\mathcal{M}}} \quad (8)$$

where \dot{m}_{array} is the total mass flow through all of the open CFVs (*i.e.*, CFVs with the end caps removed). The theoretical mass flow for a CFV array is analogous to Eq. 2:

$$\dot{m}_{th,array} = \frac{A_{array} P_0 C^* \sqrt{\mathcal{M}}}{\sqrt{R_u T_0}}, \quad (9)$$

with the exception that A_{array} is the total throat area of all of the open CFVs

$$A_{array} = \sum_{n=1}^N A_n \delta_n. \quad (10)$$

Here, $A_n = \pi d_n^2 / 4$ is the throat area of the n^{th} CFV, and δ_n is the selector function

$$\delta_n = \begin{cases} 1 & \text{uncapped CFVs} \\ 0 & \text{capped CFV} \end{cases} \quad (11)$$

which equals unity if the end cap is removed and equals zero if the end cap is fastened. For example, in Fig. 5D the selector function is unity for CFVs 18 and 19, and zero for the remaining CFVs.

The mass flow (\dot{m}_{array}) through the CFV array can be 1) measured directly using an appropriate reference standard (*e.g.*, the 26 m³ PVTt standard), or 2) computed indirectly using prior calibration results of the uncapped CFVs in the array. When using the latter approach, we assume that each CFV in the array is not influenced by neighboring CFVs (*i.e.*, no interference effects) so that the total mass flow is the sum of all of the uncapped CFVs. Moreover, the local mass flow through each uncapped CFV is determined by multiplying its fitted discharge coefficient (C_d^{FIT}) from Eq. 6 with the theoretical mass flow (\dot{m}_{th}) from Eq. 2. When the latter approach is used the CFV array discharge coefficient in Eq. 8 simplifies to

$$C_{d,array}^* = \frac{\sum_{n=1}^N C_{d,n}^{\text{FIT}} A_n \delta_n}{\sum_{n=1}^N A_n \delta_n} \quad (12)$$

the area weighted average of the fitted discharge coefficients (C_d^{FIT}) of each uncapped CFV. Here, the asterisk “*” distinguishes between the *fitted* array discharge coefficient in Eq. 12 (which does not account for possible interference effects) and the *measured* array discharge coefficient in Eq. 8.

CFV Interference Effects

Combining multiple CFVs in a parallel array as shown in Fig. 5 is a convenient way to increase the rangeability of CFV flow meters. However, the ISO 9300 international standard [2] only provides installation requirements for a single CFV. Several researchers [15, 16, 17] have studied CFV array installations for gas flow measurement applications. The focus of these studies has been to determine the interference effects caused by placing the CFVs too close together.

In 1986 Stevens showed that interference effects are negligible (*i.e.*, below 0.01 %) for toroidal throat nozzles with spacing larger than $L/d \geq 4.36$ [15] where L is the distance between the centers of two adjacent nozzles (see Fig. 5A) and d is the CFV

throat diameter. For the NIST CFV array, $(L/d)_{\text{NIST}} = 6.15$ which exceeds Steven's criterion. Nevertheless, NIST performed two additional experiments to verify that interference effects were negligible for the NIST CFV array. In both experiments the interference parameter (ξ) is used to quantify the change in mass flow attributed to interference effects.

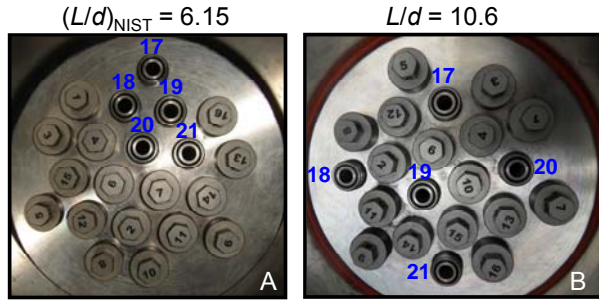


Figure 6. Spacing of 5 CFVs (*i.e.*, #'s 17, 18, 19, 20, and 21) installed in the nozzle holder: A) $(L/d)_{\text{NIST}} = 6.15$, and B) $L/d = 10.6$.

First Interference Experiment

First, we measured ξ as a function of the CFV spacing. Five CFVs were separated by $(L/d)_{\text{NIST}} = 6.15$ as shown in Fig. 6A and then separated by $L/d = 10.6$ as shown in Fig. 6B. The 26 m³ PVTt standard was used to measure $C_{d,\text{array}}$ in both configurations. For this experiment the interference parameter is defined by

$$\xi = \frac{(C_{d,\text{array}})_{L/d=6.15}}{(C_{d,\text{array}})_{L/d=10.6}} - 1 \quad (13)$$

where the subscripts denote the separations. Significant departures of ξ from zero indicates that interference effects are significant for these spacings. Because we used the same flow standard (*i.e.*, the 26 m³ PVTt system) for both configurations, the bias from errors in the flow standard did not affect the measurement of the interference parameter ξ .

The results of the interference experiment are plotted versus $1/\sqrt{Re_d}$ in Fig. 7.⁴ Figure 7A shows that the $C_{d,\text{array}}$ measurements of the five CFVs separated by $(L/d)_{\text{NIST}} = 6.15$ (▲) nearly overlap with measurements made of the five CFVs separated by

$(L/d) = 10.6$ (◆). The uncertainty bars in the figure are calculated using Eq. 16 in section 5. The interference parameter is computed using Eq. 13 and plotted as a percentage in Fig. 7B. The average value of the interference parameter (expressed as a percentage) is $\xi = 0.006\% \pm 0.015\%$ where the second number (0.015%) is twice the standard deviation. This low value for the interference parameter is on the same order as the expected reproducibility of the 26 m³ PVTt standard, which historically is 0.02% or less. Based on the small value of ξ we conclude that interference effects are negligible.

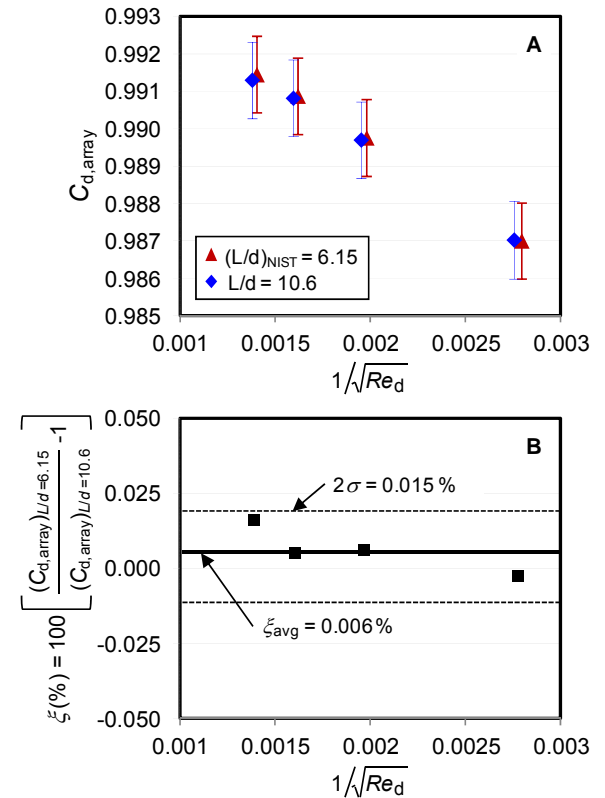


Figure 7. First interference experiment: A) $C_{d,\text{array}}$ measurements for 5 CFVs installed in parallel separated by $(L/d)_{\text{NIST}} = 6.15$ (▲) as shown in Fig. 6A, and by $L/d = 10.6$ (◆) as shown in Fig. 6B, and B) Percent difference in $C_{d,\text{array}}$ (*i.e.*, interference parameter, ξ).

Second Interference Experiment

In the second experiment the interference parameter is defined by

$$\xi = \frac{\dot{m}_{XY}}{\dot{m}_X + \dot{m}_Y} - 1, \quad (14a)$$

⁴ The diameter of a single CFV ($d = 0.205$ inch) is used as the length scale in the Reynolds number definition.

where \dot{m}_{XY} is the total mass flow from two CFVs X and Y in parallel shown in Fig. 8. Here the CFVs are taken to be choked at stagnation conditions of P_0 and T_0 . The mass flow \dot{m}_X is the mass flow that would flow through X at the same conditions with Y capped (*i.e.*, no flow), and \dot{m}_Y is the mass flow through Y with X capped (*i.e.*, no flow).

The mass flows \dot{m}_X and \dot{m}_Y are calculated using prior calibration history of CFVs X and Y. In particular, before starting the interference test CFVs X and Y are each calibrated individually, and their measured discharge coefficients are fit to the functional form in Eq. 6 (*i.e.*, $C_{d,X}^{FIT}$ and $C_{d,Y}^{FIT}$). During the interference experiment the fitted discharge coefficients are used in conjunction with Eq. 1 to determine $\dot{m}_X = C_{d,X}^{FIT} \dot{m}_{th,X}$ and $\dot{m}_Y = C_{d,Y}^{FIT} \dot{m}_{th,Y}$. On the other hand, the total mass flow \dot{m}_{XY} is measured during the interference test at the same conditions using the same flow standard used to calibrate CFVs X and Y individually. In this way the interference parameter is independent of any multiplicative (or linear flow scale up) biases introduced by the flow standard.

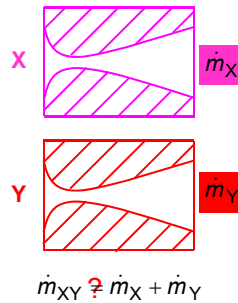


Figure 8. Mass flow from two CFVs X and Y

The interference parameter in Eq. 14a can also be expressed as

$$\xi = \frac{C_{d,array}}{C_{d,array}^*} - 1 \quad (14b)$$

where the mass flow ratio has been replaced by $C_{d,array}$ in Eq. 8 divided by $C_{d,array}^*$ in Eq. 12. Equation 14b is derived by using Eqs. 1 and 8

which relate mass flow to the discharge coefficient for a single CFV and for an array of CFVs.⁵

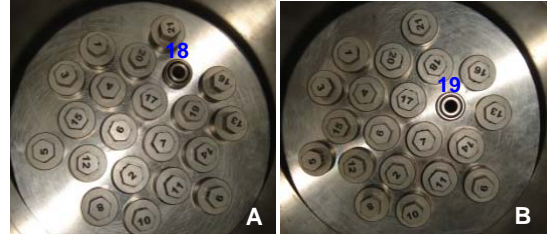


Figure 9. Configuration used to calibrate CFVs 18 and 19 individually on the 26 m³ PVTt standard.

The 26 m³ PVTt standard was used 1) to measure $C_{d,array}$ with both CFVs uncapped, and 2) to calibrate CFV 18 and CFV 19 individually. The single CFV configurations are shown in Fig. 9 and the double configuration is shown in Fig. 5D. Each CFV was individually calibrated twice almost two years apart.⁶ The respective curve fits for CFV 18 and CFV 19 use the data from both calibrations, and the standard deviation of the fit residuals are 0.008 % for CFV 18 and 0.012 % for CFV 19. The fit residuals are an indication of the long term reproducibility of the CFVs.

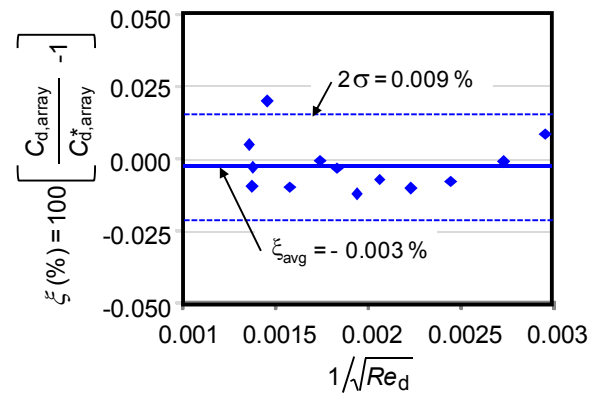


Figure 10. Interference parameter plotted against $1/\sqrt{Re_d}$ for CFVs 18 and 19 in configurations shown in Fig. 5D and Fig. 9.

⁵ Note that the ratio of theoretical mass flow for a single CFV and a CFV array equals the throat area ratio of the single CFV to the CFV array (*i.e.*, $\dot{m}_{th,A}/\dot{m}_{th,AB} = A_A/A_{AB}$ and $\dot{m}_{th,A}/\dot{m}_{th,AB} = A_A/A_{AB}$).

⁶ CFV 18 was calibrated on 3/27/2009 and again on 1/12/2011 while CFV 19 was calibrated on 4/19/2009 and a second time on 3/1/2011.

The results of the interference experiment are shown in Fig. 10. The average value of the interference parameter (expressed as a percentage) is only 0.003 %. The dashed lines show a variation of two standard deviations equal to $2\sigma = 0.009\%$. Interference effects are less than the reproducibility of the $26\text{ m}^3\text{ PVTt}$ standard and therefore too small to be detected in these measurements.

5. Comparison Results between the 677 L and $26\text{ m}^3\text{ PVTt}$ Standards Using CFV Array as Transfer Standard

Having demonstrated that interference effects are negligible, we used the CFV array as a transfer standard to compare NIST's 677 L and $26\text{ m}^3\text{ PVTt}$ standards. Here, we compare $C_{d,array}$ in Eq. 8

measured by the $26\text{ m}^3\text{ PVTt}$ standard with $C_{d,array}^*$ computed via Eq. 12 using the calibration history of the 21 CFVs calibrated on the 677 L $PVTt$ standard. Table 2 shows the flow range and CFVs used in the comparison. We assessed the level of agreement between the two $PVTt$ standards using the standardized degree of equivalence [18, 19]

$$E_n = \frac{C_{d,array} - C_{d,array}^*}{\sqrt{U_e^2(C_{d,array}) + U_e^2(C_{d,array}^*)}} \quad (15)$$

where $U_e(C_{d,array})$ and $U_e(C_{d,array}^*)$ are respectively the expanded uncertainties of the measured and fitted array discharge coefficients. The measured array discharge coefficient $U_e(C_{d,array})$ is determined via propagation of uncertainty [13, 14]

$$\frac{U_e(C_{d,array})}{C_{d,array}} = 2 \sqrt{\left[\frac{u(\dot{m})}{\dot{m}} \right]^2 + \left[\frac{u(P_0)}{P_0} \right]^2 + \frac{1}{4} \left[\frac{u(T_0)}{T_0} \right]^2 + \sigma_{\text{reprd}}^2} \quad (16)$$

where $[u(\dot{m})/\dot{m}] = 0.045\%$ is the standard mass flow uncertainty of the $26\text{ m}^3\text{ PVTt}$ standard, $[u(P_0)/P_0] = 0.02\%$ and $[u(T_0)/T_0] = 0.03\%$ are the standard uncertainties of stagnation pressure and temperature respectively, and σ_{reprd} is the standard deviation of repeated measurements at each set point. The air was dried to dew point temperatures of 243 K or less so that the uncertainty attributed to moisture contributed negligible uncertainty (*i.e.*, less than 0.007 %).

The uncertainty of the fitted array discharge coefficient is

$$\frac{U_e(C_{d,array}^*)}{C_{d,array}^*} = 2 \sum_{n=1}^N \delta_n w_n \left[\frac{u(C_{d,n}^{\text{FIT}})}{C_{d,n}^{\text{FIT}}} \right] \quad (17a)$$

where $u(C_{d,n}^{\text{FIT}})$ is taken to be perfectly correlated for all of the CFVs since 1) all of the CFVs were calibrated on the same $PVTt$ standard, and 2) this engineering assumption yields the most conservative uncertainty estimate. The weighting factor in Eq. 17a is

$$w_n = \frac{A_n}{\sum_{k=1}^N \delta_k A_k} = \frac{A_n}{A_{\text{tot}}} \quad (17b)$$

the ratio of the throat area of the n^{th} CFV and the total throat area (A_{tot}) of all of the uncapped CFVs.

Table 2. Flow range and CFVs used to compare 677 L and $26\text{ m}^3\text{ PVTt}$ standards

No. []	Flow Range		# CFVs in parallel []	List of CFVs Used (Unused CFVs are capped) []
	[slm]	[kg/s]		
1	490 to 2050	0.01 to 0.04	1	18
	420 to 2030	0.008 to 0.04	1	19
2	840 to 4100	0.08 to 0.17	2	18 & 19
3	2450 to 9450	0.05 to 0.2	5	17, 18, 19, 20, 21
4	4900 to 19700	0.1 to 0.4	10	1, 3, 4, 13, 16, 17, 18, 19, 20, 21
5	10300 to 40400	0.2 to 0.81	21	1 through 21

The comparison results are considered metrologically equivalent within the stated uncertainties when $|E_n| < 1$. Figure 11 shows the comparison results corresponding to the flow range and CFV configurations specified in Table 2. In all

cases the normalized degree of equivalence is significantly less than unity, thereby indicating that the measurement results are fully equivalent. Moreover, repeated calibrations show the stability of the CFV array and of the two *PVTt* systems.

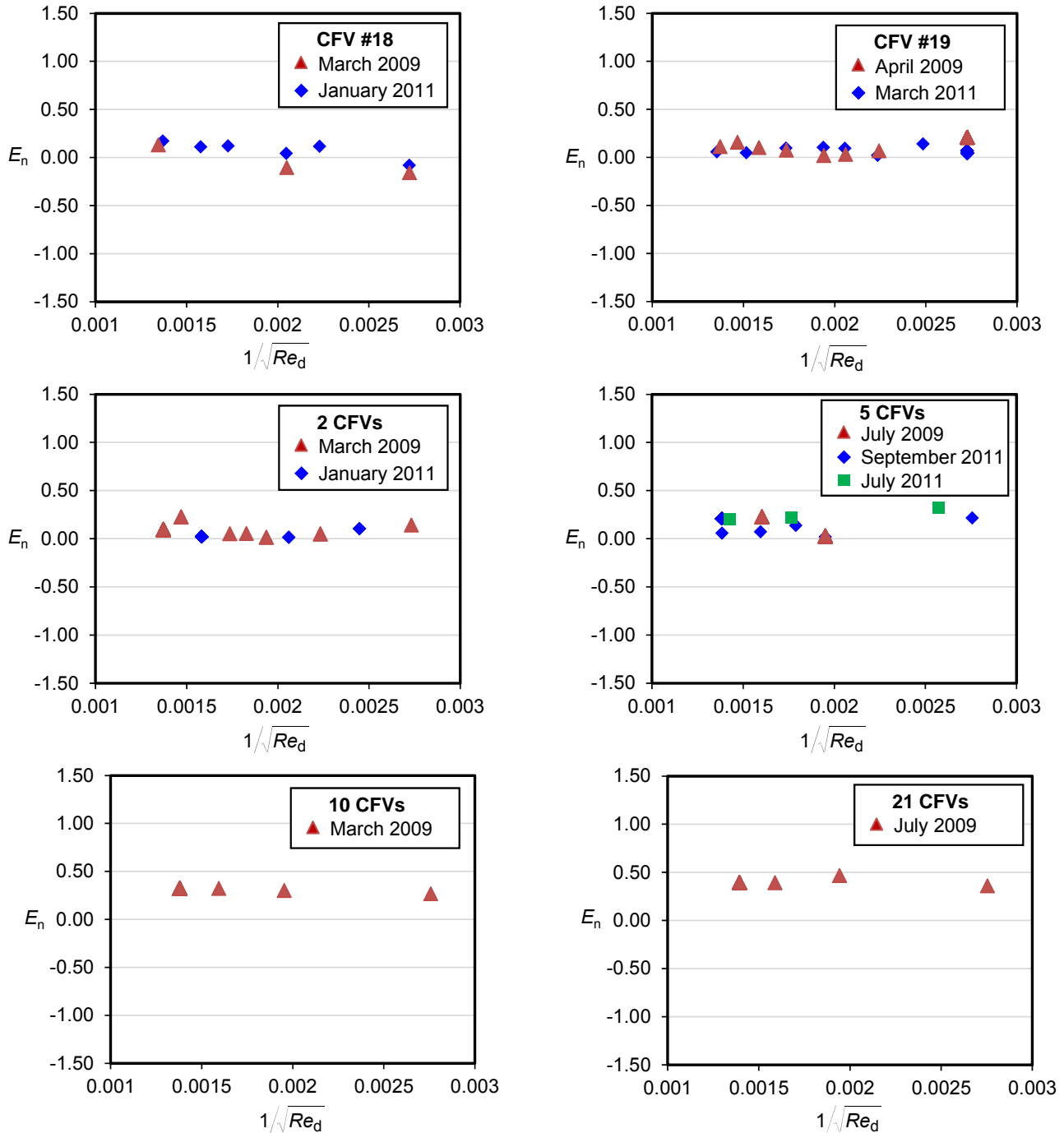


Figure 11. Comparison results between 677 L and 26 m³ *PVTt* standards which plot the standard degree of equivalence (E_n) versus inverse square root of Reynolds number⁴.

6. Practical Considerations: Periodically Cleaning the CFVs to Maintain Stability

Flow metrology applications require the CFV array to have good reproducibility. We characterized the reproducibility of all 21 CFVs by calibrating them multiple times against the 677 L *PVTt* standard over a three year period. These results, which were summarized in Table 1, are included in the uncertainty of the CFV array. However, we found it necessary to ultrasonically or manually clean the interior wall of select CFVs to maintain this level of reproducibility. In particular, those CFVs in the nozzle holder (see Fig. 5) that were not used for flow calibrations (*i.e.*, remained capped so flow stagnated in the CFV) required periodic cleaning.

Many of NIST's calibrations use only the lower flow range of the CFV array. These calibrations are performed using less than half of the 21 CFVs. The lowest uncertainty CFVs from Table 1 are used to perform all flow calibrations unless additional CFVs are required to reach the full scale flow of the meter being calibrated. Consequently, more than half of the CFVs in the array were never used, and have been capped since being installed into the nozzle holder (see Fig. 5). We surmise that these capped CFVs functionally behave as stagnation points and are susceptible to collecting oil, dirt, particles, etc. along the interior wall.

Particles that collect or build-up on the CFV wall can change the CFV calibration curve 1) by decreasing the effective throat area, and 2) by inducing transition to turbulence at a Reynolds numbers lower than expected. Both of these effects would cause a decrease in the measured C_d values. A smaller effective throat area would uniformly shift the entire calibration curve to lower C_d values, while an early transition to turbulence would cause a non-uniform shift of the calibration curve. In particular, prior to transition the calibration curve would be unchanged, but after the onset of transition the differences in the calibration curve attributed to particulate build-up would become significant.

The recalibration results of the capped CFVs (before cleaning) supported the particle build-up hypothesis. At low Reynolds numbers the calibration curves were slightly lower (*i.e.*, 0.05 %

or less) than the initial calibration curves while at higher Reynolds numbers the difference increased to as large as 0.35 % for one CFV. However, after cleaning the CFVs either 1) ultrasonically using a soapy water solution or 2) manually by vigorously rubbing the interior wall using a cotton swab saturated with ethyl alcohol, the calibration curves of all the *dirty* CFVs returned to their initial calibration values.

To avoid using dirty CFVs in calibrations, NIST installed a five micron filter in the air supply reservoir upstream of the CFV array. Additionally, before every calibration each CFV is manually cleaned with an ethyl alcohol swab. Finally, after collecting all of the calibration data using one group of CFVs, whenever possible, a second, independent group is used at selected set points to verify the results. Even with the cleaning and verification procedures, maintaining the CFV array is much easier than maintaining a primary standard.

7. Summary and Conclusions

We described a CFV array that is used as a working standard to calibrate customers' flow meters. The CFV array will be used in place of NIST's 26 m³ *PVTt* system over a flow range extending from 400 slm to 43000 slm. The uncertainty of the CFV array ranges from 0.074 % to 0.097 % depending on the flow, which is comparable to or better than the 26 m³ *PVTt* system. Moreover, the CFV array requires substantially less maintenance and performs calibrations in one-tenth of the time as the primary standard. Secondary laboratories can realize substantial benefits by switching from primary standards to working standard CFVs [20].

Each of the 21 CFVs in the array have been characterized multiple times over three years using NIST's 677 L *PVTt* standard. The manuscript demonstrates that there are no significant interference effects between neighboring CFVs in the array. Finally, the CFV array is used as a transfer standard to compare the 677 L and 26 m³ *PVTt* standards. The results show that both standards yield equivalent results within their stated uncertainties with agreement < 0.059 %.

References

- [1] Wright J. D. and Johnson A. N., *NIST Lowers Gas Flow Uncertainties to 0.025 % or Less, International Measure*, Vol. 5, pp. 30 to 39, March 2010.
- [2] International Standards Organization, *Measurement of Gas Flow by Means of Critical Flow Venturi Nozzles*, **ISO 9300:2005(E)**.
- [3] Johnson A. N. and Wright J. D., *Revised Uncertainty Analysis of NIST 26 m³ PVTt Flow Standard*, **Proc. of the International Symposium on Fluid Flow Measurement**, Queretaro, Mexico, 2006.
- [4] Wright J. D., Johnson A. N., Moldover M. R., and Kline G. M., *Gas Flowmeter Calibrations with the 34 L and 677 L PVTt Standards*, **NIST Special Publication 250-63**, 2009.
- [5] Johnson A. N. and Wright J. D., *Gas Flowmeter Calibrations with the 26 m³ PVTt Standard*, **NIST Special Publication 250-1046**, 2009.
- [6] Johnson A. N., Wright J. D. Moldover M. R., and Espina P. I., *Temperature Characterization in the Collection Tank of the NIST 26 m³ PVTt Gas Flow Standard*, **Metrologia**, 40, pp. 211 to 216, 2003.
- [7] Anderson J. D., *Modern Compressible Flow: With Historical Perspective*, **McGraw-Hill Publishers**, 1990.
- [8] Johnson A. N., and Johansen B., *Comparison of Five Natural Gas Equations of State used for Flow and Energy Measurement*, **Proc. of the 7th ISFFM**, Anchorage Alaska, July 2009.
- [9] Johnson R. C., *Calculations of Real-Gas Effects in Flow Through Critical Nozzles*, **Journal of Basic Engineering**, September 1964, pp. 519. Anchorage Alaska, July 2009.
- [10] Moldover M. R., Trusler J. P. M., Edwards T. J., Mehl J. B., and Davis R. S., *Measurement of the Universal Gas Constant R Using a Spherical Acoustic Resonator*, **J. Res. Natl. Inst. Stand. Technol.** 93, (2), 85 to 143, (1988).
- [11] Lemmon E. W., Huber M. L., and McLinden M. O., *NIST Standard Reference Database 23: Reference Fluid Thermodynamic and Transport Properties-REFPROP, Version 8.0 National Institute of Standards and Technology, Standard Reference Data Program*, Gaithersburg, 2007.
- [12] Johnson A. N., *Natural Gas Flow Calibration Service (NGFCS)*, **NIST Special Publication 250-1081**, National Institute of Standards and Technology, Gaithersburg, MD, 2008.
- [13] Coleman H. W., and Steele W. G., *Experimentation and Uncertainty Analysis for Engineers*, **John Wiley and Sons, Inc.**, New York, NY, 1989.
- [14] Taylor, B. N. and Kuyatt C. E., *Guidelines for the Evaluating and Expressing the Uncertainty of NIST Measurement Results*, **NIST Technical Note-1297**, 1994.
- [15] Stevens R. L., *Development and calibration of Boeing 18 kg/s airflow calibration transfer standard*, **Proceedings of 1st International Symposium on Fluid Flow Measurement**, 1986.
- [16] Choi Y. M., Park K. A., Park J. T., Choi H. M., and Park S. O., *Interference effects of three sonic nozzles of different throat diameters in the same meter tube*, **Flow Measurement and Instrumentation**, Volume 10, pp. 175 to 181, 1999.
- [17] Choi Y. M., Park K. A., and Park S. O., *Interference effect between sonic nozzles*, **Flow Measurement and Instrumentation** Volume 8, Issue 2, pp. 113–119, June 1998.
- [18] Cox M. G., *The Evaluation of Key Comparison Data*, **Metrologia**, 39, pp. 589 to 595, 2002.
- [19] Dopheide D. et al., *CCM.FF-KC5a: Comparison of Flow Rates for Natural Gas at High Pressure*, **Metrologia** 43, 2006.
- [20] Carter M., Johansen W., and Britton C., *Performance of a Gas Flow Meter Calibration System Using Critical Flow Venturi Standards*, **J. Metrology Soc. of India**, 26, pp. 247 to 254, 2011.